Clinical, Cosmetic and Investigational Dermatology

Dovepress
Taylor & Francis Group

Open Access Full Text Article

ORIGINAL RESEARCH

A *Ganoderma lucidum* Extract Improves Mitochondrial Function in Aging Skin and Promotes Wound Healing

Li Tao[1,2,*], Meiling Tai[3,*], Zhuang Zhou[3], Zhenwen Chen[1], Rongjinlei Zhang[1], Yuanlong Ge[1], Zhenyu Ju[1]

[1]Key Laboratory of Regenerative Medicine of Ministry of Education, Institute of Aging and Regenerative Medicine, College of Life Science and Technology, Jinan University, Guangzhou, Guangdong, People's Republic of China; [2]Department of Pathology, Guangdong Provincial People's Hospital (Guangdong Academy of Medical Sciences), Southern Medical University, Guangzhou, Guangdong, People's Republic of China; [3]R&D Center, Infinitus (China) Company Ltd, Guangzhou, Guangdong, People's Republic of China

*These authors contributed equally to this work

Correspondence: Zhenyu Ju; Yuanlong Ge, Email zhenyuju2016@jnu.edu.cn; geyuanlong@jnu.edu.cn

Purpose: This study investigates whether *Ganoderma lucidum* extract (GLE) can enhance mitochondrial function to promote wound healing in aging skin.

Methods: Natural senescent human foreskin fibroblasts (BJ) were treated with varying concentrations of GLE, and safe concentrations were determined using the cell counting kit-8 (CCK-8) assay. The levels of mitochondrial reactive oxygen species (ROS) and mitochondrial membrane potential (MMP) were measured. Animal experiments were conducted to validate GLE's effects on wound healing by assessing adenosine triphosphate (ATP) and ROS levels in skin tissues.

Results: GLE exhibited no cytotoxicity within a concentration range of 0–100 μg/mL. Simultaneously treating senescent BJ cells with 50 μg/mL or 100 μg/mL of GLE can significantly enhance cell viability. Treatment with 100 μg/mL GLE significantly increased MMP levels while reducing mitochondrial ROS levels. Hydrogel containing 2% GLE applied to injured skin promoted wound healing, increased the ATP level of the wound tissue, and decreased ROS levels in skin tissues.

Conclusion: These findings suggest that GLE can improve mitochondrial function in aging skin and promote wound healing.

Keywords: aging skin, *Ganoderma lucidum* extract, mitochondrial function, wound healing

Introduction

Cellular senescence is a fundamental biological process characterized by a profound decline in proliferative capacity and differentiation potential, ultimately leading to impaired tissue homeostasis and functional integrity.[1,2] Conspicuously, the skin serves as the most prominent outward marker of organismal aging. Which degeneration driven by both intrinsic factors such as progressive chronological changes and extrinsic factors, including ultraviolet (UV) radiation and environmental stressors.[3,4] The hallmarks of ageing skin are laxity, sagging, and the deepening of wrinkles.[5,6] Beyond these aesthetic manifestations, the visible changes in aging skin impose a substantial psychosocial burden, adversely affecting an individual's quality of life and self-perception, and often correlating with broader age-related diseases.[7] Crucially, aging skin is also functionally compromised, exhibiting a markedly diminished capacity for efficient wound healing.[8] Therefore, developing robust strategies to mitigate skin aging is paramount not only for preserving dermal health but also for enhancing psychological well-being and potentially influencing systemic aging processes.

Mitochondria are indispensable organelles, serving as central regulators of cellular bioenergetics and redox homeostasis.[9,10] Current research confirms that robust mitochondrial function is critically important for maintaining epidermal integrity and overall dermal health.[11,12] Conversely, mitochondrial dysfunction accelerates skin aging and inflammation,

https://doi.org/10.2147/CCID.S596475
Received: 2 February 2026
Accepted: 19 April 2026
Published: 30 April 2026

leading to disorders in skin physiological functions and the occurrence of skin pathologies.[12] Beyond these foundational roles, mitochondria are crucial for processes such as immune homeostasis, wound healing, hair growth, and hormone regulation in the skin.[13] A profound and reciprocal relationship exists between cellular senescence and mitochondrial damage, positioning them as key hallmarks of the aging process.[14,15] Specifically, cellular senescence often instigates mitochondrial dysfunction, characterized by diminished oxidative phosphorylation efficiency, reduced ATP synthesis, and a decline in mitochondrial membrane potential, frequently accompanied by an overproduction of ROS. This subsequent accumulation of ROS induces pervasive oxidative stress within mitochondrial and cellular components, thereby creating a vicious cycle that ultimately exacerbates and drives cellular senescence.[16,17]

Ganoderma lucidum, a renowned medicinal mushroom in Traditional Chinese Medicine, is described in the classic literature as *Shen Nong Ben Cao Jing* as having rejuvenated and life-prolonging properties. Chemical analyses have identified a diverse array of over 200 bioactive compounds within *Ganoderma lucidum*, including polysaccharides, triterpenes, sterols, alkaloids, proteins, and nucleotides.[18] Extensive pharmacological research has subsequently elucidated numerous beneficial activities attributed to *Ganoderma lucidum*, encompassing antioxidant, anti-inflammatory, immunomodulatory, anti-aging, hepatoprotective, and anti-allergic effects.[19,20] Building upon this rich traditional use and established pharmacological profile, this study aims to investigate whether a GLE can enhance the mitochondrial function of senescent BJ cells and promote wound healing in aged skin.

Materials and Methods

Experimental Animals

All experimental procedures were conducted in accordance with LACU guidelines and were approved by the Ethics Committee of Jinan University (approval number: 20221227–17). Male C57BL/6J mice (2-months-old) were obtained from GemPharmatech Biotechnology Company (Guangdong, China).

All animals were housed in an environment maintained at a temperature of 22 ± 1 °C, a relative humidity of 50 ± 1%, and a 12/12-hour light/dark cycle, with free access to water and food. All mice were acclimatized and fed in the aforementioned environment for one week prior to the start of the experiment.

Mice were irradiated with 4.5 Gy twice (once monthly) to establish a mouse skin ageing model. A total of 20 mice were irradiated. They were then randomly assigned to the control group, the 1% GLE treatment group and the 2% GLE treatment group.

The mice were anesthetized by a single intraperitoneal injection of 180 mg/kg of tribromoethanol (Cat#T48402, Sigma Aldrich, USA), and the back skin was shaved before the wound experiments. To prevent other mice from causing further injury to the wound, all mice were housed individually following shaving and surgery.

After treating the skin with 75% alcohol, a 6-millimetre full-thickness skin wound was made under sterile conditions. Full-thickness skin wounds were created in mice using a 6 mm diameter sterile biopsy punch. Control hydrogel or GLE-containing hydrogel (1% and 2%) was applied to the wound. Observe and photograph the healing progress of the wound. The mice were euthanized by cervical dislocation, which was followed the American Veterinary Medical Association guidelines. Collect skin wound specimens frozen at −80°C or fixed in paraformaldehyde for subsequent experimental investigation.

Preparation of the Cordyceps sinensis Hydrogel

The hydrogel was prepared by heating and mixing an aqueous phase (containing deionized water, glycerin, and gelling agents) with a lipid phase (comprising meadowfoam seed oil, shea butter, and emulsifiers) at 78–80°C. Following vacuum homogenization to form a uniform emulsion base, the mixture was cooled below 45°C, and *Cordyceps sinensis* extract (total triterpenes and sterols at a concentration of ≥ 20%, and Ganoderma polysaccharides at ≥ 400 mg/kg) was incorporated to obtain the final hydrogel.

Hematoxylin-Eosin (H&E) Staining

Fresh skin tissue was fixed in 4% paraformaldehyde for 24 hours, followed by stepwise dehydration in alcohol. Subsequently, the skin tissue was placed in paraffin and subjected to fixation treatment. The wax-embedded skin tissue

blocks were cut into 4μm thick skin tissue sections for subsequent experiments. After the skin tissue sections were deparaffinized, the nuclei were stained with hematoxylin and the cytoplasm was stained with eosin. After the staining process was completed, the skin tissue sections were dehydrated and mounted, and then scanned using a panoramic scanner (3D HISTECH, Hungary) to obtain high-resolution images for subsequent observation and analysis.

Cell Culture and Treatment

BJ cells were obtained from the American Type Culture Collection (ATCC). They were cultured in high glucose DMEM medium (Gibco, USA) supplemented with 10% foetal bovine serum (ExCell Bio, China), 100 U/mL penicillin, and 100 μg/mL streptomycin (Invitrogen, USA). BJ cells were cultured to passage 40 for senescent cells (SEN) and before passage 30 for young cells (Young). GLE is supplied by Infinitus (China) Co., Ltd. Senescent BJ cells were treated with varying concentrations (0–100 μg/mL) of GLE, were chosen based on cell viability assays which showed optimal efficacy without cytotoxicity.

CCK-8 Assay

Cell viability of BJ cells was assessed using the CCK-8 assay (Beyotime, China). BJ cells were seeded in a 96-well plate at a density of 5000 cells per well and treat with varying concentrations (0–100 μg/mL) of GLE. Subsequently, add 10 μL of CCK-8 reagent to each well and incubate the culture plate in the dark at 37°C with 5% CO_2 for 1 hour. Measure the optical density in the wells using a microplate reader (Synergy HTX, BioTek, USA).

ROS, Mitochondrial ROS and MMP Detection

Fresh skin tissues from mice were collected and prepared into cell suspensions using a grinding pestle. The levels of ROS in cells were evaluated using the DCFH-DA probe (Beyotime, China). Mitochondrial ROS levels were assessed using MitoROS probe (AAT Bioquest, USA). MMP levels were assessed using TMRE probe (Beyotime, China). Collect cell suspensions or BJ cells and incubate them separately with DCFH-DA, MitoROS or TMRE probes at 37°C for 30 minutes. Following incubation, the cells were washed with PBS, then stained with DAPI to exclude dead cells. To account for background autofluorescence, unstained cells (without probes) were included as negative controls in all experiments. Sample were analysed using a BD LSRFortessa™ flow cytometer. The gating strategy was strictly applied to ensure data reliability: cell debris was first excluded based on forward scatter (FSC-A) and side scatter (SSC-A), followed by doublet discrimination (singlet gating) using FSC-A versus FSC-H. Finally, viable cells were selected by gating out DAPI-positive dead cells. The fluorescence signals of the respective probes were quantified exclusively from the viable singlet population and expressed as Mean Fluorescence Intensity.

ATP Content

The ATP concentration in the skin tissue was detected using an ATP detection kit (Beyotime, China). The skin tissue was lysed according to the manufacturer's instructions. The lysate of the skin tissue was collected, centrifuged, and 20 μL of the supernatant was taken for ATP measurement. The ATP content was measured using a microplate reader (Synergy HTX, BioTek, USA).

NAD+ Measurement

Skin and BJ cell samples were collected, and NAD+/NADH was extracted using a commercial kit (Cat#S0175, Beyotime, China) in accordance with the manufacturer's instructions. The supernatant obtained from the extraction was transferred to a 96-well plate, thoroughly mixed with an ethanol dehydrogenase working solution, and incubated at 37°C in the dark for 10 minutes. Subsequently, add 10 μL of color development solution to each well, mix thoroughly, incubate at 37°C in the dark for 10 minutes, and measure the absorbance at 450 nm using a microplate reader. Use the following equation for the calculation: [NAD+] = [NADtotal] – [NADH].

RNA Extraction and Quantitative Real-Time PCR

TRIzol reagent (Cat#9109, Takara, Japan) was used to extract total RNA from BJ cells. The concentration and purity of the RNA were determined using a NanoDrop system. Subsequently, 1 μg of total RNA was used for reverse transcription using HiScriptIII

Reverse Transcriptase (Cat#R323-01, Vazyme, China). Quantitative reverse transcription PCR (qRT-PCR) was performed on an Applied Biosystems QuantStudio 6 real-time qPCR System (Applied Biosystems, USA) using RealStar Power SYBR qPCR Mix (Cat#A314-10, GenStar, China). The primer sequences are as follows: β-actin-F 5'-CCAACCGCGAGAAGATGA-3', β-actin-R 5'-TCCATCACGATGCCAGTG-3'; FUNDC1-F 5'- CCACAGTTCGGGACCTATGG −3', FUNDC1-R 5'- AGCCAC TATGACTAGCAATCTGA −3'; Parkin-F 5'- CCAGAGGAAAGTCACCTGCGAA −3', Parkin-R 5'- CTGAGGCTTCAAA TACGGCACTG −3'; PINK1-F 5'- GCCTCATCGAGGAAAAACAGG −3', PINK1-R 5'- GTCTCGTGTCCAACGGGTC −3'; ULK1-F 5'- AGCACGATTTGGAGGTCGC −3', ULK1-R 5'- GCCACGATGTTTTCATGTTTCA −3'; ATG5-F 5'- AA AGATGTGCTTCGAGATGTGT −3', ATG5-R 5'- CACTTTGTCAGTTACCAACGTCA −3'; LC3B-F 5'- GAGAAGCAGC TTCCTGTTCTGG −3', LC3B-R 5'- GTGTCCGTTCACCAACAGGAAG −3'; β-actin-M-F 5'- GGCTGTATTCCCCTCCA TCG-3', β-actin-M-R 5'- CCAGTTGGTAACAATGCCATGT-3'; p16-M-F 5'- CGCAGGTTCTTGGTCACTGT-3', p16-M-R 5'- TGTTCACGAAAGCCAGAGCG-3'. The relative expression levels of each gene were calculated using the $2^{(-\Delta\Delta CT)}$ formula.

Senescence-Associated β-Galactosidase (SA-β-Gal) Staining

Cellular senescence was assessed using an SA-β-gal staining kit (Catalog No. C0602, beyotime) according to the manufacturer's instructions. Briefly, BJ cells were washed with PBS, fixed for 15 min at room temperature, and incubated with the SA-β-gal staining solution overnight at 37 °C without CO_2. The senescent cells, identified by blue cytoplasmic staining, were observed and photographed under an inverted microscope. The percentage of SA-β-gal positive cells was quantified using ImageJ software from at least three randomly selected fields per well.

Statistical Analysis

FlowJo software was used to analyze the flow cytometry data. Image J software was used to analysis images. All data are presented as the mean ± standard deviation (SD). Student's unpaired two-tailed *t*-test or one-way ANOVA with Tukey's multiple comparison test were used for statistical analysis. Ns indicates not significant, *P < 0.05, **P < 0.01, ***P < 0.001, ****P < 0.0001. Analyses were performed using Graphpad Prism software.

Results

GLE and Its Monomer Components Exhibit Excellent Biocompatibility

To evaluate the biocompatibility of *Ganoderma lucidum* extract and its monomeric components, a Cell Counting Kit 8 (CCK-8) assay was performed on BJ cells. The results demonstrated that all five tested concentrations of GLE and its monomeric components were well-tolerated, showing no evidence of cytotoxicity (Figure 1A–C). Based on these dose-response findings, concentrations of 50 μg/mL and 100 μg/mL of GLE were selected for subsequent mechanistic studies (Figure 1A). Collectively, these results confirm that GLE and its monomeric components exhibit excellent biocompatibility.

GLE Promotes Wound Healing in Skin of Aged Mouse

Having confirmed the safety of GLE, its role in the wound healing process was further investigated. First, a mouse model of accelerated skin ageing will be established using an irradiation model. Subsequently, 6-millimetre-diameter skin wounds were created on the backs of the experimental mice exhibiting skin ageing, and the wounds were treated with carrier hydrogel, 1% or 2% GLE hydrogel, respectively, to modulate the wound healing process (Figure 2A). To determine skin aging in mice after irradiation, it was measured the expression of the p16 gene in skin tissues. The results showed that p16 expression was significantly upregulated in the skin of irradiated mice (Figure 2B). The results demonstrated that skin treated with the 2% GLE hydrogel exhibited significantly accelerated healing, resulting in markedly smaller wound areas by Day 8 post-wounding compared to the control group (Figure 2C and D). H&E staining of skin tissue near the wounds on day 8 showed that the wound structure in GLE-treated mice was more complete, as shown in Figure 2E and F. Collectively, these findings suggest that Ganoderma extract promotes wound healing in aged mice.

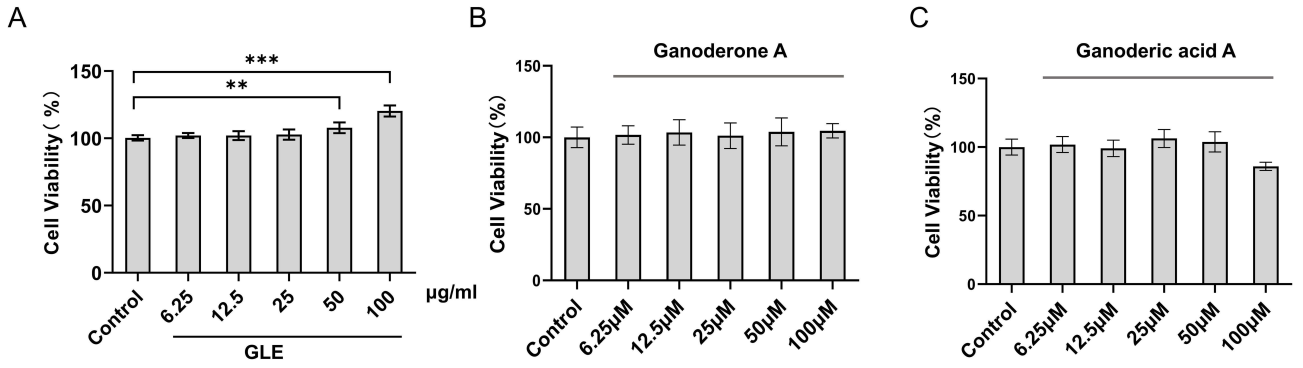

Figure 1 GLE and Its Monomer Components Exhibit Excellent Biocompatibility. (**A**) The effect of GLE on the cell viability of senescent BJ cells was determined using the CCK-8 method. Data represents mean ± SD, one-way ANOVA with Tukey's multiple comparison test were used for statistical analysis; **P < 0.01, ***P < 0.001. (**B**) The effect of Ganoderone A on the cell viability of senescent BJ cells was determined using the CCK-8 method. (**C**) The effect of Ganoderic acid A on the cell viability of senescent BJ cells was determined using the CCK-8 method.

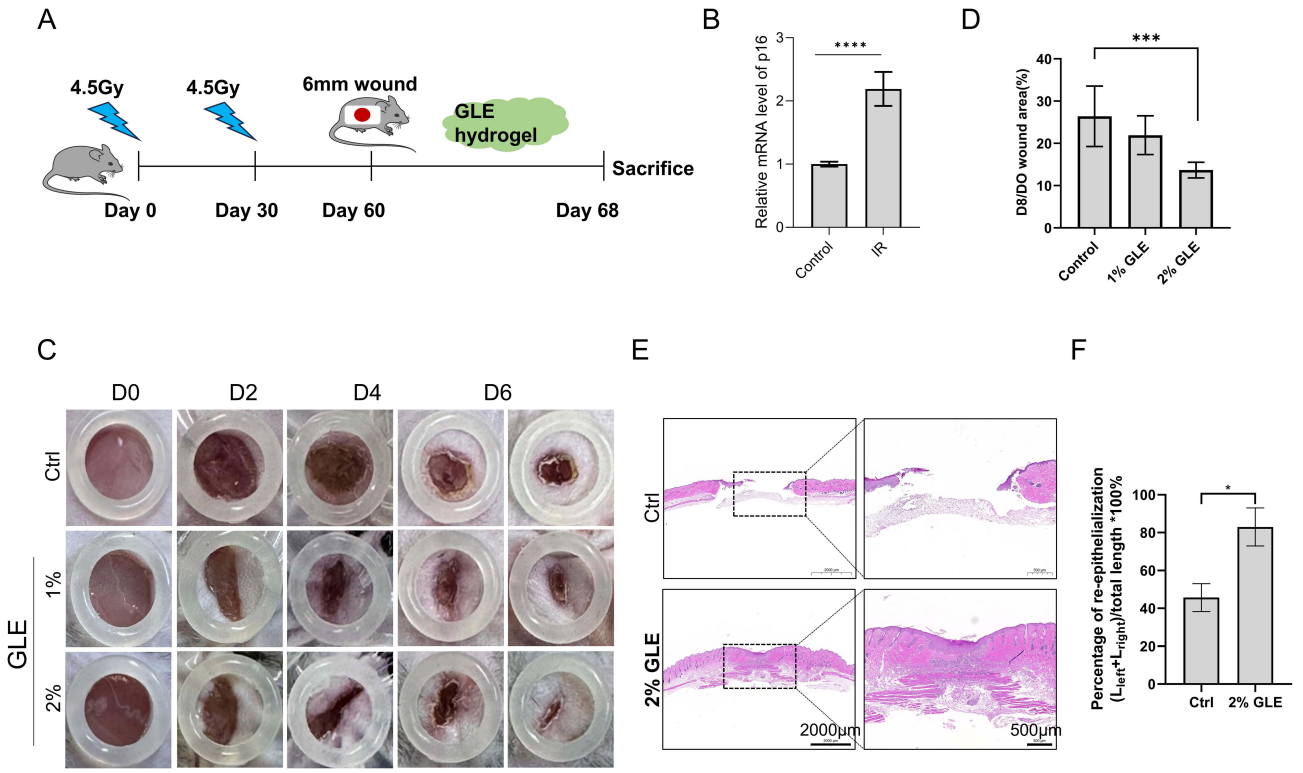

Figure 2 GLE Promoted Wound Healing in Skin of Aged Mouse. (**A**) Construction of a mouse model of skin aging and schematic diagram of the intervention process for aging skin wounds. (**B**) p16 mRNA levels were quantified by qPCR. n = 3 independent experiments. Data represents mean ± SD, Student's unpaired two-tailed *t*-test were used for statistical analysis; ****P < 0.0001. (**C**) Take photos to observe and record the healing process of aging skin wounds. (**D**) Calculate the percentage of wound area (D8/D0) using the ImageJ software, n = 3–7 mice/group. Data represents mean ± SD, one-way ANOVA with Tukey's multiple comparison test were used for statistical analysis; ***P < 0.001. (**E**) The histological changes of the wound tissue on day 8 were observed using H&E staining. (**F**) Quantitative histomorphometry of E using ImageJ software. The lengths of the newly formed migrating epithelial tongues extending from both the left and right wound margins (defined by the cessation of hair follicles) were measured. The sum of these lengths was then divided by the original wound width to determine the re-epithelialization percentage, *P < 0.05.

GLE Reduces Mitochondrial ROS in Senescent BJ Cells

Having demonstrated that GLE promotes wound healing in aged mouse skin, the underlying mechanisms of GLE will be investigated further. Elevated levels of ROS are a hallmark of senescent cells and represent a major contributor to cellular oxidative stress, leading to structural damage and functional impairment. Initially, the levels of total ROS in BJ cells following GLE treatment were measured; however, no significant changes were observed (Figure 3A and B). Considering that mitochondria are particularly susceptible to damage caused by ROS, which can disrupt their function and compromise cellular integrity, the

https://doi.org/10.2147/CCID.S596475

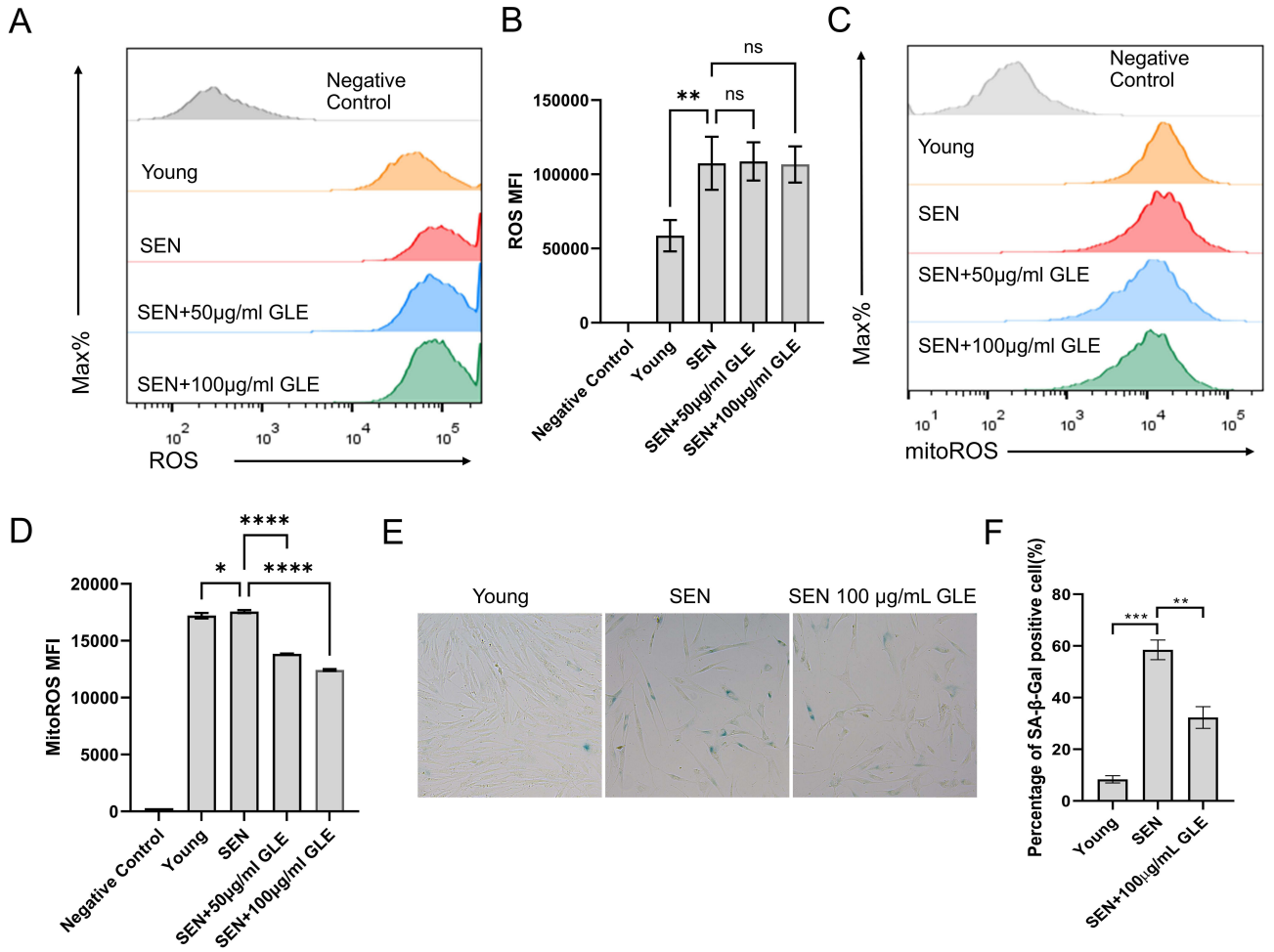

Figure 3 GLE reduces mitochondrial ROS level in senescent BJ cells. (**A** and **B**) The ROS probe was used to investigate the effect of GLE on the total ROS levels of BJ cells, n = 3 independent experiments. Data represents mean ± SD, one-way ANOVA with Tukey's multiple comparison test were used for statistical analysis; ns, not significant, $^{**}P < 0.01$. (**C** and **D**) The MitoRos probe was used to investigate the effect of GLE on the mitochondrial ROS levels of BJ cells, n = 3 independent experiments. (**E**) Representative images of SA-β-gal staining in young BJ cells, senescent BJ cells, and senescent BJ cells treated with GLE. (**F**) Quantitative analysis of the percentage of SA-β-gal positive cells across the different groups. Data represents mean ± SD, one-way ANOVA with Tukey's multiple comparison test were used for statistical analysis; $^{*}P < 0.05$, $^{**}P < 0.01$, $^{***}P < 0.001$, $^{****}P < 0.0001$.

levels of mitochondrial ROS from senescent BJ cells were specifically measured. Treatment with GLE (50 or 100 μg/mL) significantly reduced mitochondrial ROS levels in a dose-dependent manner (Figure 3C and D). To validate the establishment of cellular senescence and robustly evaluate the anti-senescent efficacy of GLE, SA-β-gal staining was performed. As depicted in Figure 3E and F, senescent BJ cells exhibited a significantly higher percentage of SA-β-gal positive staining compared to young, confirming the successful senescent phenotype. Notably, following treatment with GLE, the proportion of SA-β-gal positive cells was markedly reduced. These phenotypic assessments directly demonstrate that GLE effectively ameliorates cellular senescence in BJ cells. These findings suggest that the therapeutic effects of GLE in promoting wound healing in aged skin may be attributed, at least in part, to its role in enhancing mitochondrial function and attenuating mitochondrial ROS accumulation.

GLE Enhances ATP Levels and Reduced ROS in Aging Skin and Senescent Cell

In addition to assessing ROS levels in senescent BJ cells, ROS levels were also examined in the skin of ageing mice. Consistent with the cellular findings, ROS levels in aging dermal tissue were significantly reduced following GLE treatment (Figure 4A). Given that the production of ATP is a key function of mitochondria, ATP levels were subsequently measured in aged mouse skin. Dermal ATP levels were markedly elevated in mice treated with 2% GLE hydrogel compared to the control group (Figure 4B).

https://doi.org/10.2147/CCID.S596475

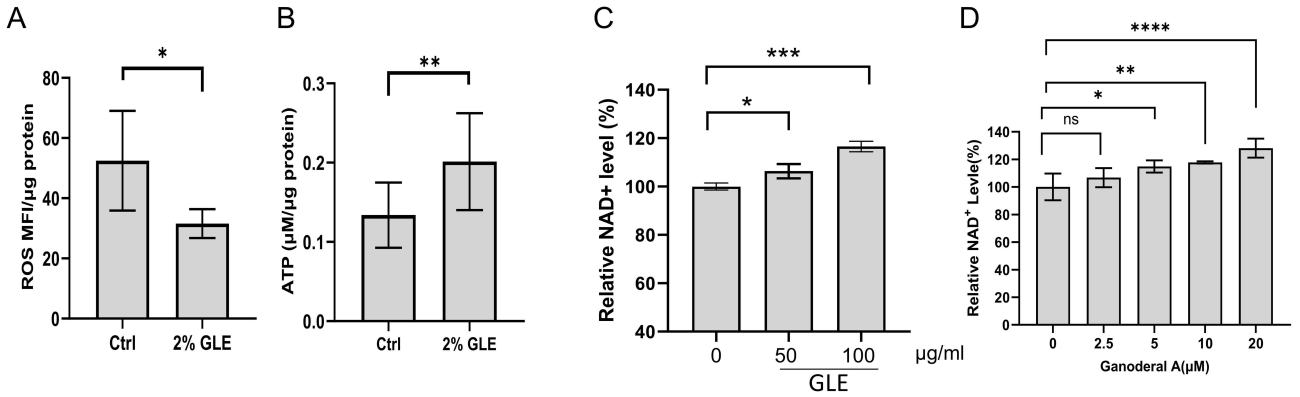

Figure 4 GLE Enhances ATP Levels and Reduced ROS in Aging Skin and senescent cell. (**A**) Using the DCFH-DA probe to investigate the effect of GLE on the ROS levels in aged skin wounds, n = 4 mice/group. Data represents mean ± SD, Student's unpaired two-tailed *t*-test were used for statistical analysis; *P < 0.05. (**B**) Obtain the tissue from the wound on day 8 and investigate the effect of GLE on the ATP levels in aged skin wounds, n = 4 mice/group. Data represents mean ± SD, Student's unpaired two-tailed *t*-test were used for statistical analysis; **P < 0.01. (**C**) Detect the NAD^+ levels after GLE treatment on BJ cells, n = 3 independent experiments. Data represents mean ± SD, one-way ANOVA with Tukey's multiple comparison test were used for statistical analysis; *P < 0.05, ***P < 0.001. (**D**) Detect the NAD^+ levels after Ganoderal A treatment on BJ cells, n = 3 independent experiments. Data represents mean ± SD, one-way ANOVA with Tukey's multiple comparison test were used for statistical analysis; ns, not significant, *P < 0.05, **P < 0.01, ***P < 0.001, ****P < 0.0001.

To further investigate the potential mechanisms underlying the increase in ATP levels, the concentration of NAD^+ was subsequently measured, as NAD^+ serves as an essential substrate for ATP generation. The results revealed that GLE treatment significantly increased NAD^+ levels in senescent cell (Figure 4C). Moreover, one of GLE's active monomeric components, Ganoderal A, exhibited a similar ability to enhance NAD^+ levels (Figure 4D). Collectively, these findings demonstrate that GLE enhances mitochondrial function through the elevation of NAD^+ levels and subsequent ATP production, while simultaneously reducing ROS accumulation in aging skin and senescent cells.

GLE Enhances MMP Levels in Senescent BJ Cells

To further evaluate mitochondrial functionality, mitochondrial membrane potential (MMP) was measured; this is a critical indicator of mitochondrial health, reflecting the functional integrity of mitochondria and their role in ATP synthesis, ion transport and redox regulation.[21] An increase in MMP indicates enhanced mitochondrial function. Treatment of senescent BJ cells with GLE (50 or 100 μg/mL) significantly elevated MMP. Notably, the 100 μg/mL GLE concentration specifically induced a 19.01% increase in MMP compared to the senescent control group, thereby demonstrating GLE's capacity to restore mitochondrial function (Figure 5A and B). This finding is consistent with our

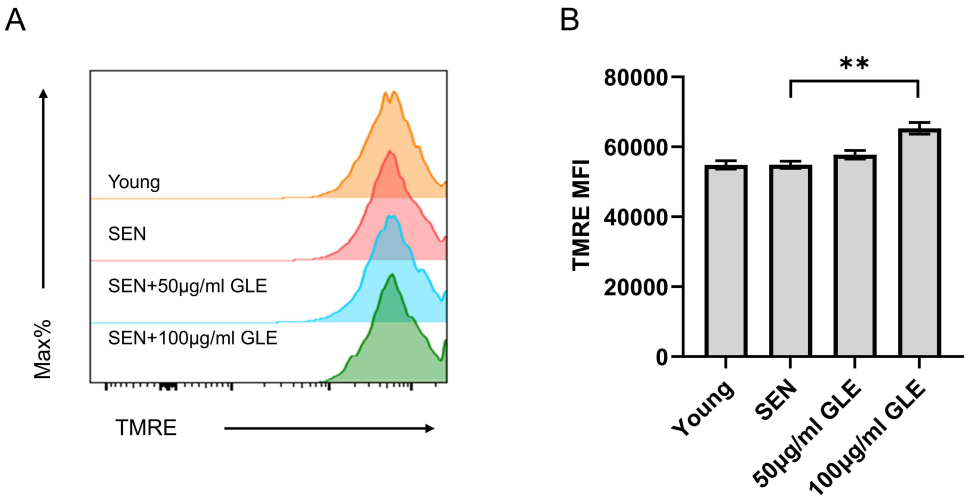

Figure 5 GLE Enhances MMP Levels in Senescent BJ cells. (**A** and **B**) Using the TMRE probe to investigate the effect of GLE on the MMP levels of senescent BJ cells, n = 3 independent experiments. Data represents mean ± SD, one-way ANOVA with Tukey's multiple comparison test were used for statistical analysis; **P < 0.01.

https://doi.org/10.2147/CCID.S596475

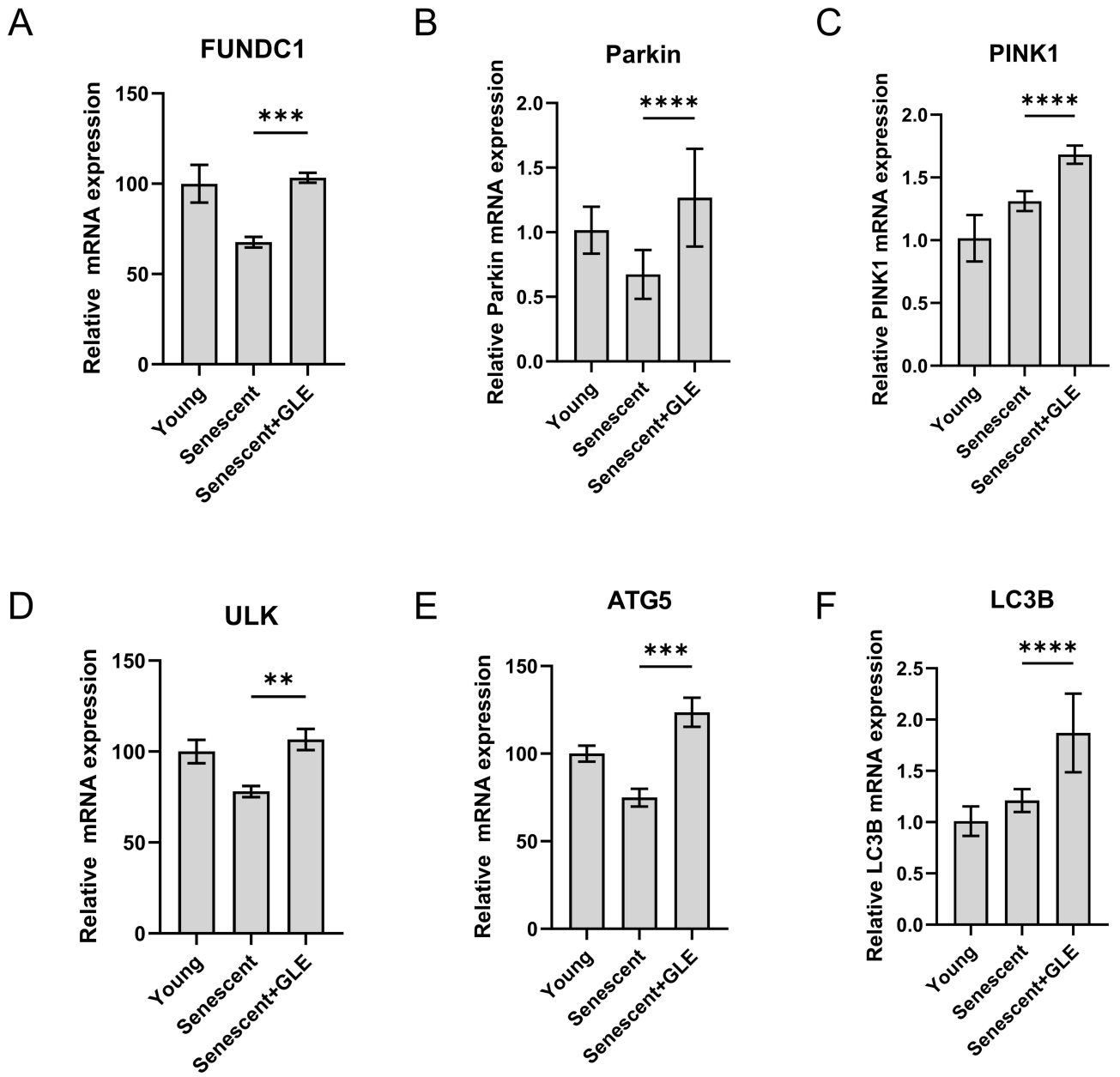

Figure 6 GLE Enhances the Autophagy Pathway. (**A**–**F**) Autophagy pathway related gene's mRNA levels were quantified by qPCR. n = 3 independent experiments. Data represents mean ± SD, one-way ANOVA with Tukey's multiple comparison test were used for statistical analysis; **P < 0.01, ***P < 0.001, ****P < 0.0001.

earlier observation of increased ATP and NAD in these cells, further underscoring GLE's capacity to enhance overall mitochondrial function.

GLE Enhances the Autophagy Pathway

Mitochondrial dysfunction and impaired autophagy are hallmark characteristics of cellular senescence. Given that the above findings indicate that GLE leads to increased levels of ATP and NAD^+, further investigations were conducted to determine how GLE influences the autophagy process. Analysis of autophagy-related signaling revealed a significant upregulation of several key genes involved in the autophagy pathway following GLE treatment (Figure 6A–F). This upregulation suggests that GLE activates the autophagy pathway, facilitating the clearance of defective mitochondria in senescent cells and, consequently, enhancing mitochondrial function.

 https://doi.org/10.2147/CCID.S596475

Discussion

Cellular senescence, particularly of dermal fibroblasts, plays a central role in the age-related decline of skin function and impaired wound healing capacity.[22,23] Senescent cells are characterized by irreversible cell cycle arrest and the secretion of senescence-associated secretory phenotypes, which collectively disrupt tissue homeostasis.[24,25] The present study demonstrates that *Ganoderma lucidum* extract significantly accelerates wound closure in an irradiation-induced premature skin aging murine model. Mechanistically, these macroscopic therapeutic benefits are underpinned by the restoration of mitochondrial bioenergetics, the reduction of oxidative stress, and the activation of the autophagy pathway in senescent fibroblasts, effectively reversing age-associated cellular dysfunction.

During the wound healing process, dermal fibroblasts are subjected to high metabolic demands, requiring substantial ATP for extracellular matrix synthesis, proliferation, and tissue remodeling.[26] In aged skin, mitochondrial dysfunction and the concomitant accumulation of ROS compromise these bioenergetic requirements, leading to delayed healing. The findings of this study reveal that GLE intervention significantly elevates intracellular NAD+ and ATP levels while restoring mitochondrial membrane potential in senescent BJ cells. Given that NAD+ is a critical co-enzyme for cellular metabolism, its upregulation by GLE likely replenishes the bioenergetic pool required for efficient fibroblast function. This in vitro mitochondrial rejuvenation directly correlates with the in vivo observations of increased dermal ATP and reduced tissue ROS, providing a clear bioenergetic mechanism for the accelerated macroscopic wound closure.

Furthermore, impaired autophagy is a hallmark of cellular senescence, inextricably linked to the accumulation of defective mitochondria and oxidative stress. The current study observed a significant upregulation of key autophagy-related genes following GLE treatment. It is well-established that enhanced autophagic flux facilitates the clearance of damaged organelles, such as dysfunctional mitochondria (mitophagy). Therefore, it is highly plausible that the GLE-induced activation of the autophagy pathway serves as an upstream regulatory mechanism that reduces mitochondrial ROS leakage and restores overall mitochondrial health. This dual action scavenging existing ROS and preventing new ROS generation through autophagic clearance highlights a comprehensive and synergistic anti-aging mechanism of GLE in dermal tissue.

Ganoderma lucidum contains a complex matrix of bioactive compounds, predominantly polysaccharides and triterpenoids, which have been extensively documented for their diverse pharmacological activities.[20,27] While previous studies have reported the efficacy of *Ganoderma lucidum* extracts in alleviating oxidative stress, modulating apoptosis, and exerting anti-inflammatory effects in various pathological contexts,[28–33] the present investigation specifically translates these properties to the context of skin aging and tissue repair. The potent antioxidant and metabolic-regulating effects observed herein are likely attributable to the synergistic actions of *Ganoderma lucidum* polysaccharides and triterpenoids. By targeting the fundamental intrinsic drivers of cellular senescence, GLE distinguishes itself from conventional single-target wound dressings, offering a holistic microenvironmental modulation for aged skin.

Despite these promising findings, several limitations must be acknowledged. First, wound healing is a highly orchestrated multicellular process. While this study focused exclusively on the intrinsic response of senescent dermal fibroblasts, the potential immunomodulatory effects of GLE on other critical skin-resident cells, such as macrophages and keratinocytes, warrant further investigation. Second, although the therapeutic efficacy of the commercial GLE was robustly demonstrated, the lack of precise quantitative phytochemical profiling (eg, via high-performance liquid chromatography) limits the ability to attribute the observed macroscopic effects to specific active monomers. Future research should aim to delineate the complete chemical fingerprint of the extract and explore the cross-talk between different skin cell types under GLE treatment, thereby accelerating its translational application in geriatric dermatology.

Conclusions

This study investigated the effects of GLE on senescent BJ cells and the wound healing process in aged skin. To this end, this study monitored changes in parameters including cell viability, MMP, mitochondrial ROS, tissue ROS levels, and tissue ATP levels. Concurrently, this study examined the wound healing process and the pathological changes at the wound site. It can be stated that GLE exerts positive effects in ameliorating BJ cell senescence and accelerating wound healing in aged skin. These beneficial actions of GLE may be attributed to its capacity to enhance mitochondrial function and downregulate ROS levels.

Our findings will provide insights for further investigations into the biological effects of GLE, and the utilization of GLE may represent an effective strategy for combating skin ageing and managing wounds healing in aged skin.

Data Sharing Statement

The data that support the findings of this study are available from the corresponding author upon reasonable request.

Acknowledgments

This research received no external funding.

Disclosure

The authors declare no conflicts of interest in this work.

References

1. Ogrodnik M. Cellular aging beyond cellular senescence: markers of senescence prior to cell cycle arrest in vitro and in vivo. *Aging Cell*. 2021;20(4):e13338. doi:10.1111/acel.13338
2. Summer R, Shaghaghi H, Schriner D, et al. Activation of the mTORC1/PGC-1 axis promotes mitochondrial biogenesis and induces cellular senescence in the lung epithelium. *Am J Physiol Lung Cell Mol Physiol*. 2019;316(6):L1049–l60. doi:10.1152/ajplung.00244.2018
3. Franco AC, Aveleira C, Cavadas C. Skin senescence: mechanisms and impact on whole-body aging. *Trends Mol Med*. 2022;28(2):97–109. doi:10.1016/j.molmed.2021.12.003
4. Naidoo K, Hanna R, Birch-Machin MA. What is the role of mitochondrial dysfunction in skin photoaging? *Experim Dermatol*. 2018;27(2):124–128. doi:10.1111/exd.13476
5. Hu SC, Lin CL, Yu HS. Dermoscopic assessment of xerosis severity, pigmentation pattern and vascular morphology in subjects with physiological aging and photoaging. *European J Dermatol*. 2019;29(3):274–280. doi:10.1684/ejd.2019.3555
6. Yaar M, Eller MS, Gilchrest BA. Fifty years of skin aging. *J Invest Dermatol Symp Proc*. 2002;7(1):51–58. doi:10.1046/j.1523-1747.2002.19636.x
7. Quan T, Li R, Gao T. Role of mitochondrial dynamics in skin homeostasis: an update. *Int J Mol Sci*. 2025;26(5):1803. doi:10.3390/ijms26051803
8. Tu H, Shi Y, Guo Y, et al. Young fibroblast-derived migrasomes alleviate keratinocyte senescence and enhance wound healing in aged skin. *J Nanobiotechnol*. 2025;23(1):200. doi:10.1186/s12951-025-03293-2
9. Wallace DC, Fan W, Procaccio V. Mitochondrial energetics and therapeutics. *Ann Rev Pathol*. 2010;5(1):297–348. doi:10.1146/annurev.pathol.4.110807.092314
10. Srivastava S. Emerging therapeutic roles for NAD(+) metabolism in mitochondrial and age-related disorders. *Clin Transl Med*. 2016;5(1):25. doi:10.1186/s40169-016-0104-7
11. Sreedhar A, Aguilera-Aguirre L, Singh KK. Mitochondria in skin health, aging, and disease. *Cell Death Dis*. 2020;11(6):444. doi:10.1038/s41419-020-2649-z
12. Martic I, Papaccio F, Bellei B, et al. Mitochondrial dynamics and metabolism across skin cells: implications for skin homeostasis and aging. *Front Physiol*. 2023;14:1284410. doi:10.3389/fphys.2023.1284410
13. Stout R, Birch-Machin M. Mitochondria's role in skin ageing. *Biology*. 2019;8(2):29. doi:10.3390/biology8020029
14. Miwa S, Kashyap S, Chini E, et al. Mitochondrial dysfunction in cell senescence and aging. *J Clin Invest*. 2022;132(13). doi:10.1172/JCI158447
15. Wu Z, Qu J, Zhang W, et al. Biomarkers of ageing of humans and non-human primates. *Nat Rev Mol Cell Biol*. 2025;26(11):826–847. doi:10.1038/s41580-025-00883-8
16. Chapman J, Fielder E, Passos JF. Mitochondrial dysfunction and cell senescence: deciphering a complex relationship. *FEBS Lett*. 2019;593(13):1566–1579. doi:10.1002/1873-3468.13498
17. Gao X, Yu X, Zhang C, et al. Telomeres and mitochondrial metabolism: implications for cellular senescence and age-related diseases. *Stem Cell Rev Rep*. 2022;18(7):2315–2327. doi:10.1007/s12015-022-10370-8
18. Liu Y, Ren S, Sang Q, et al. Potential active compounds of *Ganoderma lucidum* and their anticancer effects: a comprehensive review. *Food Sci Nutr*. 2025;13(8):e70741. doi:10.1002/fsn3.70741
19. Li C, Zhang R, Tian B, et al. A review of the extraction technologies, structural characterization, chemical modification, and pharmacological effects of *Ganoderma lucidum* polysaccharides. *Naunyn-Schmiedeberg's Arch Pharmacol*. 2025;398(12):16967–16998. doi:10.1007/s00210-025-04436-w
20. Ren S, Liu H, Sang Q, et al. A review of bioactive components and pharmacological effects of *Ganoderma lucidum*. *Food Sci Nutr*. 2025;13(7):e70623. doi:10.1002/fsn3.70623
21. Zorova LD, Popkov VA, Plotnikov EY, et al. Mitochondrial membrane potential. *Anal Biochem*. 2018;552:50–59. doi:10.1016/j.ab.2017.07.009
22. Mchugh D, Gil J. Senescence and aging: causes, consequences, and therapeutic avenues. *J Cell Biol*. 2018;217(1):65–77. doi:10.1083/jcb.201708092
23. Jipu R, Serban IL, Goriuc A, et al. Targeting dermal fibroblast senescence: from cellular plasticity to anti-aging therapies. *Biomedicines*. 2025;13(8):1927. doi:10.3390/biomedicines13081927
24. Hayflick L, Moorhead PS. The serial cultivation of human diploid cell strains. *Exp Cell Res*. 1961;25(3):585–621. doi:10.1016/0014-4827(61)90192-6
25. Campisi J, D'adda Di Fagagna F. Cellular senescence: when bad things happen to good cells. *Nat Rev Mol Cell Biol*. 2007;8(9):729–740. doi:10.1038/nrm2233
26. Zorina A, Zorin V, Kudlay D, et al. Age-related changes in the fibroblastic differon of the dermis: role in skin aging. *Int J Mol Sci*. 2022;23(11):6135. doi:10.3390/ijms23116135

27. Qin X, Fang Z, Zhang J, et al. Regulatory effect of *Ganoderma lucidum* and its active components on gut flora in diseases. *Front Microbiol*. 2024;15:1362479. doi:10.3389/fmicb.2024.1362479
28. Raza SHA, Zhong R, Li X, et al. *Ganoderma lucidum* triterpenoids investigating their role in medicinal applications and genomic protection. *J Pharm Pharmacol*. 2024;76(12):1535–1551. doi:10.1093/jpp/rgae133
29. Li X, Wu Q, Bu M, et al. Ergosterol peroxide activates Foxo3-mediated cell death signaling by inhibiting AKT and c-Myc in human hepatocellular carcinoma cells. *Oncotarget*. 2016;7(23):33948–33959. doi:10.18632/oncotarget.8608
30. Xu J, Xiao C, Xu H, et al. Anti-inflammatory effects of *Ganoderma lucidum* sterols via attenuation of the p38 MAPK and NF-κB pathways in LPS-induced RAW 264.7 macrophages. *Food Chem Toxicol*. 2021;150:112073. doi:10.1016/j.fct.2021.112073
31. Ahmad MF. *Ganoderma lucidum*: persuasive biologically active constituents and their health endorsement. *Biomed Pharmacother*. 2018;107:507–519. doi:10.1016/j.biopha.2018.08.036
32. Fu Y, Shi L, Ding K. Structure elucidation and anti-tumor activity in vivo of a polysaccharide from spores of *Ganoderma lucidum* (Fr.) Karst. *Int J Biol Macromol*. 2019;141:693–699. doi:10.1016/j.ijbiomac.2019.09.046
33. Zhu XL, Chen AF, Lin ZB. *Ganoderma lucidum* polysaccharides enhance the function of immunological effector cells in immunosuppressed mice. *J Ethnopharmacol*. 2007;111(2):219–226. doi:10.1016/j.jep.2006.11.013